Case Study Project Report

on

Visualization of the Bubble and its Growth, along with Mixing Phenomenon in Multi-Jet Fluidized Bed

By- Shivam Swarnakar

Visvesvaraya National Institute of Technology, Nagpur 440010

1. Introduction:

Fluidized bed is an important and widely acceptable process in various range of industries. In fluidized bed there are generally two phases or in some cases multiple phases are interacting together. In fluidized bed, solid phase is made to behave like a fluid by passing liquid or gas through it. This process is known as fluidization. Geometrically, fluidized bed is a chamber in which solid particles are present in static condition until gas is passed through it from the bottom of the fluidized bed. Fluidized bed is preferred in industries because it provides high area of contact between two phases, which allows higher heat transfer rates, mass transfer rate and uniform mixing, which results in low temperature gradient. Fluidized beds are highly used in chemical and petroleum industries for conducting gas-solid chemical reaction i.e. gasification of coal, gas-solid catalytic reaction i.e. catalytic cracking of petroleum and also used in bioreactors.

1.1 Fluidization Regimes

In fluidization, solid particles are made to behave like a fluid by passing gas or liquid with certain velocity. As the velocity is changed different types of fluidization regimes are developed in fluidized bed. At low velocity, the drag force is very less to lift up the particles, and it's called as fixed bed. When the velocity increases sufficiently to lift up the particles; this is the onset of minimum fluidization velocity. Increasing the velocity further will lead to bubble formation; this is called as bubbling fluidized bed. As the velocity is further increased bubble are formed, which collapse into other bubbles and results in the formation of larger bubbles and if the height to diameter ratio of fluidized bed is high enough then this causes the slugging bed formation. If the velocity of gas further increased and it exceeds the terminal velocity of the particles then the bed surface will disappear and causes turbulent bed formation. Further increasing the velocity will lead to development of pneumatic transport of solid. Figure 1.1 shows the various fluidization regimes.

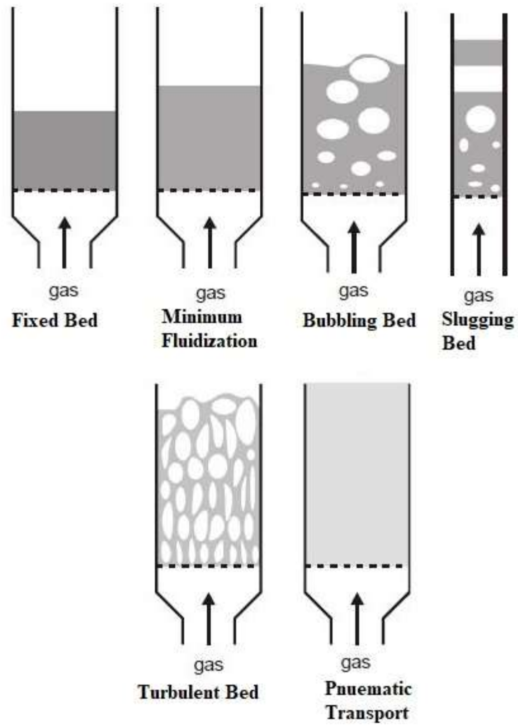

Figure 1.1: Fluidization regimes based on magnitude of velocities

2. Methodology:

In numerical methods there are two ways to simulate the two-phase fluidised bed using computational fluid dynamics. The simulation of two phase flow of gas-solid can is done with Euler – Euler method (Two Fluid Method) and Lagrange – Eulerian method.

Euler-Euler approach will be used for solving multi-jet fluidized bed. In Euler – Euler method both phases are considered as interpenetrating continua, which provides a good balance between computational cost and accuracy in the description of the flow. Navier–Stokes equations are solved for both phase and are closed with momentum transfer models along with kinetic friction models for description of granular phase. While in Lagrange – Euler method, equations of motion are solved for discrete phase so that precise interaction of solid-solid and solid-gas phases can be described. But Lagrange- Euler method costs more because of high computational needs. For simulation purpose OpenFOAM version

4.0 is used and the solver selected is twoPhaseEulerFOAM. And for meshing ICEM CFD is used. Post processing is done on paraView.

3. Governing Equations

Continuity equation for gas phase is given by Eq. (1) where, α_g is the gas phase fraction and ρ_g is the gas density and U_g is the gas velocity:

$$\frac{d\alpha_g\rho_g}{dt} + \nabla.\left(\alpha_g\rho_g U_g\right) = 0 \tag{1}$$

Similarly for solid phase fraction continuity equation is given by Eq. (2) where, α_s is the gas phase fraction and ρ_s is the solid density and U_s is the solid velocity:

$$\frac{d\alpha_s\rho_s}{dt} + \nabla.\left(\alpha_s\rho_s U_s\right) = 0 \tag{2}$$

The gas phase momentum equation is given by Eq. (3), where the gas phase stress tensor is calculated according to Newton's expression of Eq. (4):

$$\frac{d(\alpha_g\rho_g U_g)}{dt} + \nabla.\left(\alpha_g\rho_g U_g U_g\right) = \nabla.\tau_g - \alpha_g\nabla p + \alpha_g\rho_g g - K_{drag}(U_g - U_s) \tag{3}$$

$$\tau_g = \mu_g[\nabla U_g + \nabla^T U_g] - \frac{2}{3}\mu_g\left(\nabla.U_g\right)I \tag{4}$$

In particle phase momentum equation Eq. (5) an additional term is added i.e. gradient of particle pressure P_s , according to model A [17]. The particle phase stress tensor is given by Eq. (6):

$$\frac{d(\alpha_s\rho_s U_s)}{dt} + \nabla.\left(\alpha_s\rho_s U_s U_s\right) = \nabla.\tau_s - \alpha_s\nabla p - \nabla P_s + \alpha_s\rho_s g - K_{drag}(U_g - U_s) \tag{5}$$

$$\tau_s = \mu_s[\nabla U_s + \nabla^T U_s] - (\lambda_s - \frac{2}{3}\mu_s)\left(\nabla.U_g\right)I \tag{6}$$

4. Test Case Description

Figure 4.1 (a) shows the 2D schematic representation of the multi-jet fluidized bed. It has three jets of width 0.0127m at the base of the fluidized bed which allows jet to be introduced in the bed while the rest of the bed introduces gas with a minimum fluidization velocity. Fluidized bed has height of 0.5844m and width of 0.6m. The static bed height of

0.3m and initial solid volume fraction is 0.598. Density of solid particle is 2610 kg/m^3 and gas density is 1.2 kg/m^3. The rest of the parameters is given in Table 4.1.

Structured meshing is chosen for multi-jet because it provides better control for the nodes size and the grid is aligned in the flow direction which leads to more accuracy and better convergence in CFD solver and it also requires less computational power. The mesh size for test case is 212x180 with the spacing of 0.0009 near the jet inlets. Figure 4.1 (b) shows the mesh for the geometry.

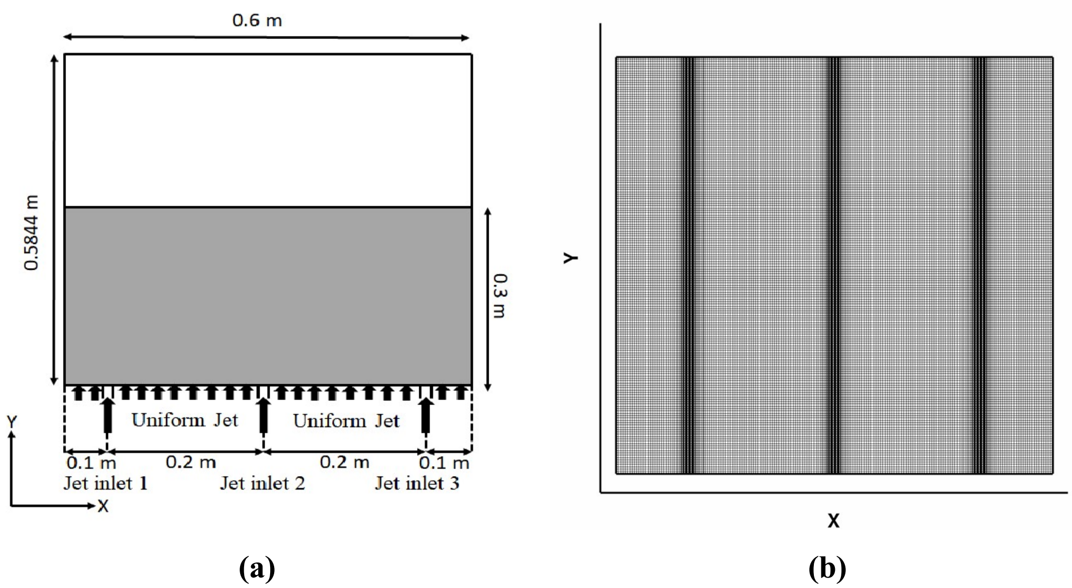

Figure 4.1: (a) Schematic representation of multi-jet fluidized bed, (b) Meshing of multi-jet fluidized bed

4.1 Boundary Condition

For gas phase, at inlet dirichlet boundary condition is given with a fixed value of velocity. In this case velocity taken for simulation is 3.550m/s. At walls dirichlet condition is assigned and at outlet mixed boundary condition is applied. For particle phase, at inlet and outlet, dirichlet condition is assigned and at walls Johnson-Jackson boundary condition is applied. Particle phase velocity in initially zero. In the Johnson-Jackson boundary condition, particle velocity at the wall is calculated from Eq. (7), where ψ is the specularity coefficient. When $\psi = 0$, free slip condition is used at the wall and when $\psi = 1$, no-slip wall condition is applied.

$$\tau_{s,w} = -\frac{\pi}{6}\frac{\alpha_s}{\alpha_{s,max}}\psi\rho_s g_0\sqrt{3\theta}U_{s,w} \quad (7)$$

For pressure, at inlet and walls, pressure gradient depend on the specified velocity condition at the boundary and at outlet atmospheric condition is applied. For granular temperature, at inlet, fixed value of 1×10^{-5} was applied and at outlet Neumann condition is used.

Table 4.1: Parameters for the simulation of fluidized bed with central jet and multi-jet

Parameters	**Value**
Domain height, m	0.6
Domain width, m	0.5844
Domain depth, m	0.0381
Bed height, m	0.3
Jet orifice width, m	0.0127
Jet orifice pitch, m	0.2
Number of jet orifice	3
Solid volume fraction	0.598
Jet inlet velocity, m/s	3.550
Minimum fluidization velocity, m/s	0.282
Gas density, kg/m^3	1.2
Gas kinematic viscosity, m^2/s	1.4×10^{-5}
Particle diameter, m	5×10^{-4}
Particle density, kg/m^3	2610
Particle-particle restitution co-efficient	0.8
Specularity co-efficient	0.5
$\alpha_{s,max}$	0.65
$\alpha_{s,min}$	0.63

4.2 Numerical Solution

Governing equations are solved using open source CFD code OpenFOAM by applying appropriate initial and boundary conditions as described in boundary condition section. SIMPLE algorithm is used for pressure-velocity coupling. Here, for the convection terms in the granular temperature transport equation, the phase momentum equations and the solid phase continuity equation - the limited-Linear, limitedLinearV and limitedLinear01 schemes are adopted respectively. The fluidized bed problems are very sensitive to the schemes selected, so utmost care should be taken while selecting schemes.

5. Validation

For validation, simulation results of fluidized bed with central jet are validated with experimental data of Gidaspow et. al. [1]. Figure 1 (a) and 1(b) shows the schematic representation of geometry used by Gidaspow [1] and meshing of the validation geometry respectively. Jet inlet velocity and minimum fluidization velocity are set to 3.55 m/s and 0.282 m/s respectively. Initially solid volume fraction of 0.598 and is given up to a height of 0.3m. All other parameters are tuned according to the Gidaspow et. al. [1] experimental setup.

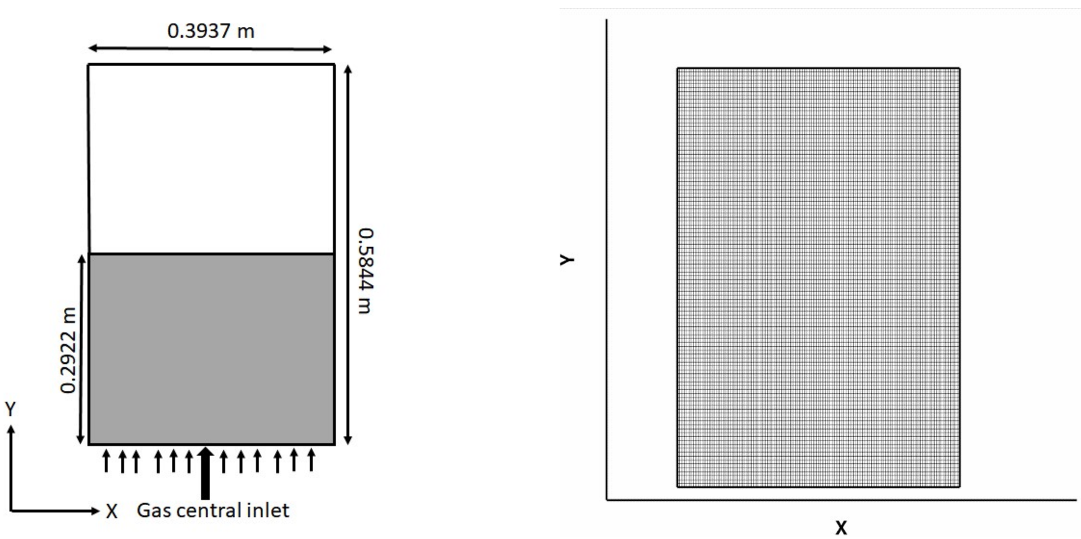

(a) **(b)**

Figure 5.1: (a) Validation geometry and (b) meshing of validation geometry

For simulation Euler-Euler method is used in OpenFOAM, which uses *twoPhaseEulerFoam* solver. Figure 2 shows the comparison of experimental results with the simulation results of the fluidized bed. Figure 2 shows the variation of the time averaged solid volume fraction in vertical direction up to height of 0.25m above the jet inlet. From figure 2 it is clear that simulation results are in good agreement with the experimental data and hence *twoPhaseEulerFoam* solver is validated.

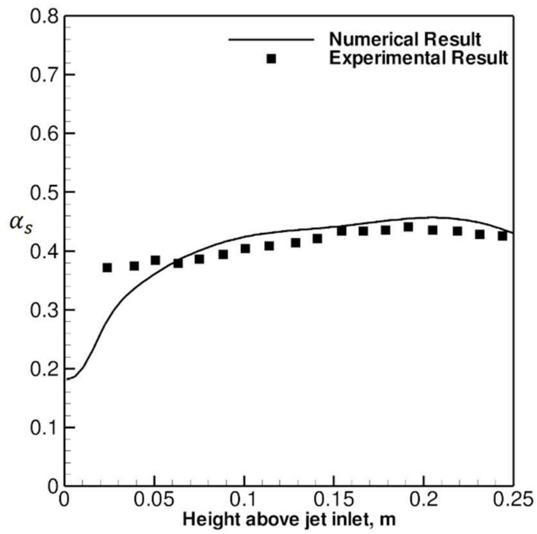

Figure5.2: Validation of the simulated results

6. Result and Discussion

In this section bubble growth, along with mixing phenomenon and effect of co-efficient of restitution is discussed.

6.1 Bubble Growth

As the high speed jet of gases passes through the jets, it creates a bubble by replacing the nearby solid particles. Bubble size also increases as it moves upward. After $t \geq 5sec$, bubbles reaches the surface and begin to burst which causes intense mixing of the two phase. After first bubble formation, only mixing happens and solid particles starts to accumulate near the solid walls.

6.2 Effect of Coefficient of restitution (e_s)

Figure 6.1-6.3 shows contours of solid volume fraction (α_s) for three values of coefficient of restitution (e_s) at various time instants. From the figure 6.1-6.3 it is observed that as the value of e increases there is decrease in bubble size and its formation. Also as the value of e_s decreases, particle become closely packed in the denser regions of the bed, resutling in the sharper porosity contours and larger bubbles. For time instant of 0.3 sec, the bubble is sharper and has its boundary well defined but as going toward higher values of e it is observed that the bubble shape gets diffused and this effect is more prominent for $e_s =$ 0.99. It happens because as the value of e_s increases particle pressure will aslo increase and will lead to the suppression of bubble formation and growth. Also as the value of

e_s increases the particle phase bulk viscosity will also increase; which means that increase in the resistance to particle phase compression

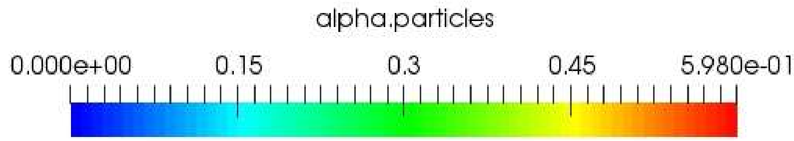

Common Legend for Figure 6.1-6.3

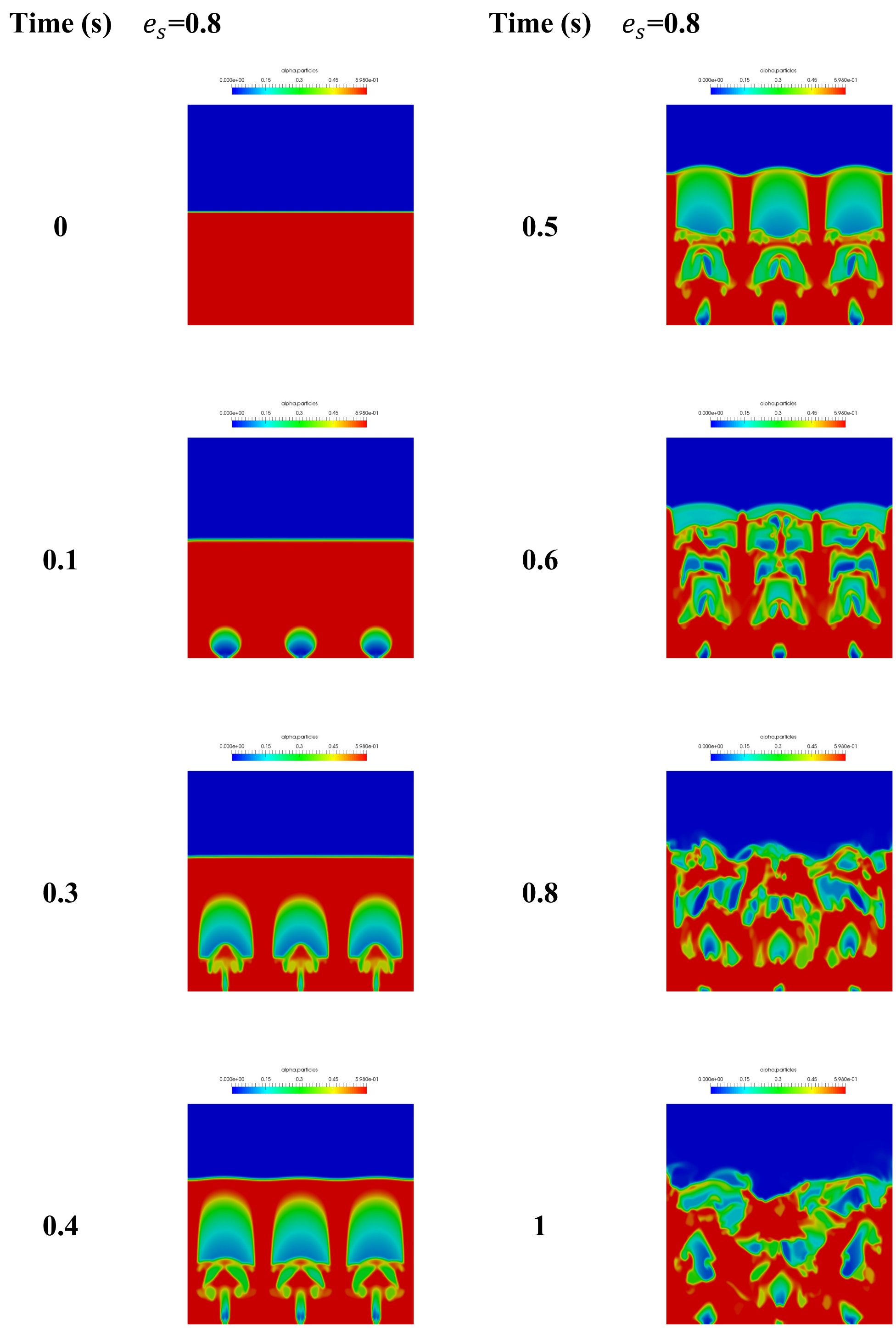

Figure 6.1: Contours of solid volume fraction (α_s) at variuos time instants for $e_s = 0.8$

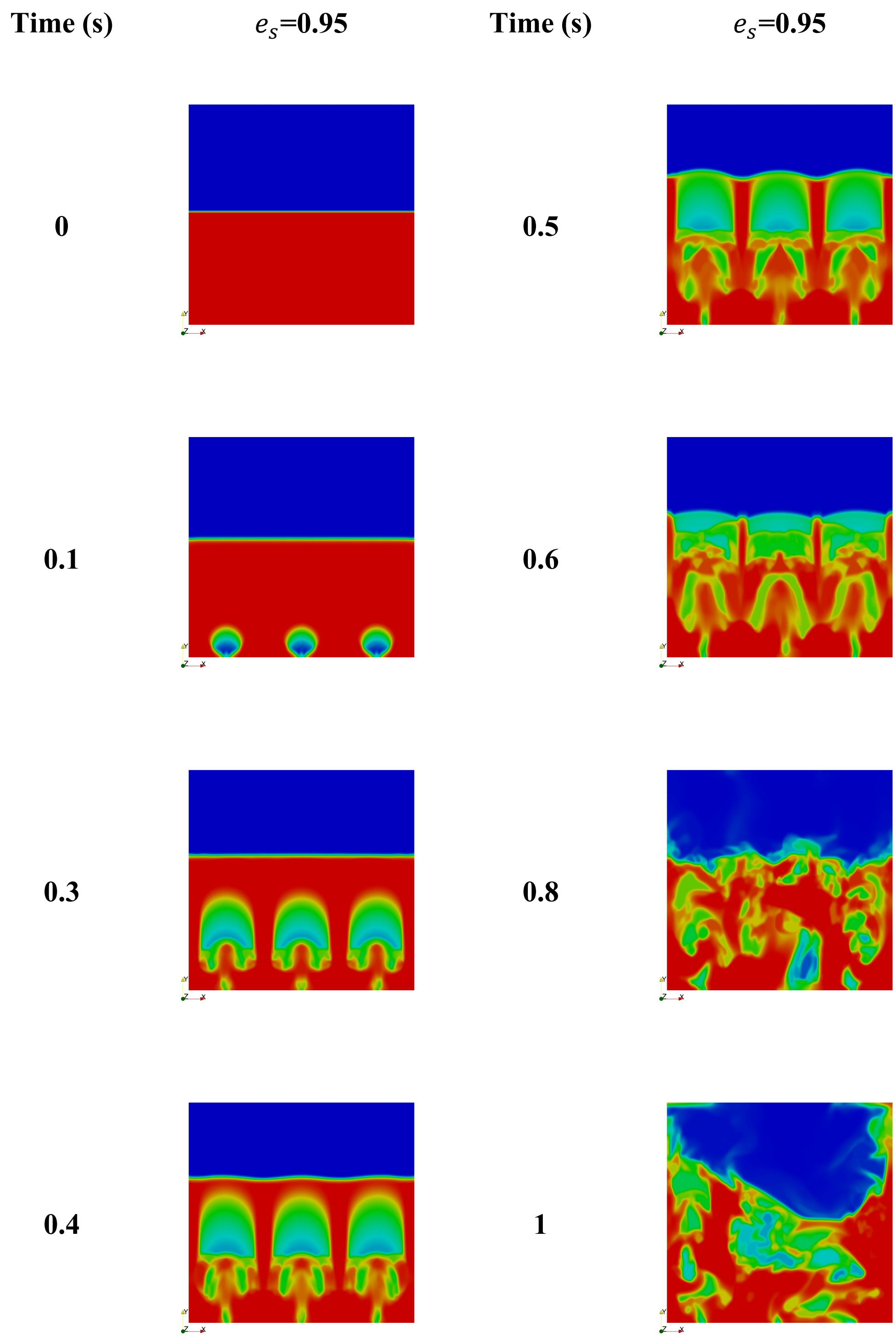

Figure 6.2: Contours of solid volume fraction (α_s) at variuos time instants for $e_s = 0.95$

Time (s)	e_s=0.99	Time (s)	e_s=0.99
0	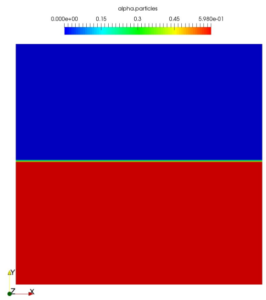	0.5	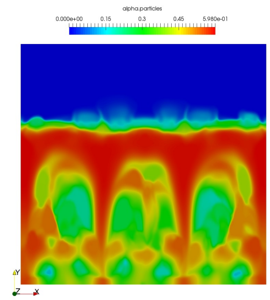
0.1	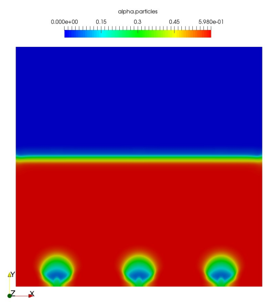	0.6	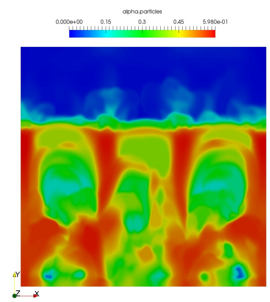
0.3	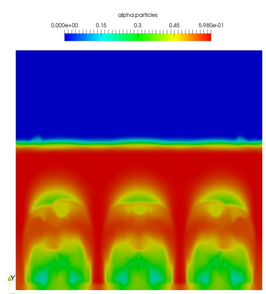	0.8	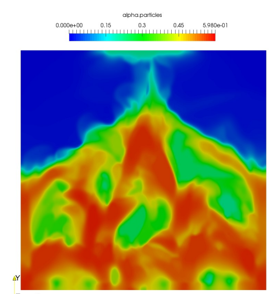
0.4	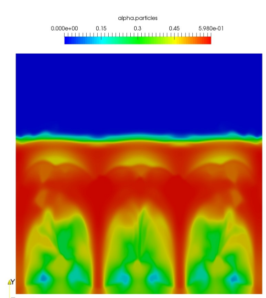	1	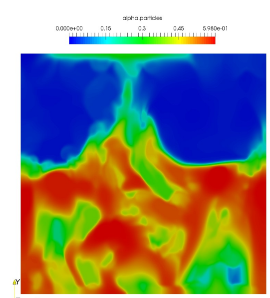

Figure 6.3: Contours of solid volume fraction (α_s) at variuos time instants for $e_s = 0.99$

7. Conclusion

In the work bubble growth along with mixing of two phase is visualised and from the results of co-efficient of restitution it is observed that the co-efficient of restitution have large influence on the bubble formation and its size. For very higher values of co-efficient of restitution i.e. close to unity, variation of solid volume fraction is found to be uniform and bubble formation stops when coefficient of restitution reaches unity.